Cholesterol-AMUPol and AMUPol for Dynamic Nuclear Polarization of Membrane Proteins

Tran, N. (U. of Florida, Chemistry); Mehta, A.K. (U. of Florida, AMRIS); Rivere, G. (U. of Florida, Biochemistry & Molecular Biology); Mentink-Vigier, F. (NHFML); Abe, S., Casano, G., Ouari, O. (Aix-Marseille U., Inst. of Radical Chemistry) and Long, J.R. (U. of Florida, Biochemistry & Molecular Biology)

Introduction

Membrane proteins pose unique challenges for MAS-DNP, requiring a radical matrix that (1) preserves the native lipid membrane environment, (2) efficiently and uniformly polarizes proteins deeply embedded in the lipid bilayer, and (3) allows standard incorporation of known radical concentrations into liposome suspensions. To date, most common biological DNP sample matrices include radical dissolved in a glassing agent (water/glycerol) solution, to hopefully allow for uniform distribution of radical throughout the entire sample. Traditional DNP radical enriched sample matrices with glassing agents are problematic for use with lipid membranes, as glassing agents (e.g. glycerol) have been shown to induce lipid interdigitation, consequently disrupting native lipid packing and membrane dynamics. Here we present DNP results at 600 MHz/395 GHz for a lung surfactant peptide mimetic, KL_4, utilizing a novel sterol lipid tethered biradical, cholesterol-AMUPol. Our hypothesis is that tethering AMUPol to cholesterol will localize the AMUPol biradical to the membrane in a way that maximizes enhancement of the peptide. The use of cholesterol-AMUPol does not require addition of glassing agent. We compare DNP efficiency, polarization, and performance between cholesterol-AMUPol and AMUPol in hydrated liposomes.

Experimental

Spectra were collected at 600 MHz/395 GHz Bruker DNP spectrometer utilizing a Bruker MAS DNP $^{1}H/^{13}C/^{15}N$ probe. MAS was set to 10 kHz for all experiments and temperature regulated at ~90K.

Results and Discussion

DNP buildup and enhancement were compared between cholesterol-AMUPol and AMUPol. We observed a more uniform signal enhancement for KL_4 and lipid resonances in the presence of cholesterol-AMUPol. A stark difference in polarization build-up and enhancement were observed for carbons of the lipid glycerol backbone, where shorter DNP buildup time (~2.4 sec) and larger enhancement (ε~20) was measured in the presence of AMUPol compared to cholesterol-AMUPol (~4.5 sec DNP buildup and enhancement ε~14). We hypothesize AMUPol partitions at the membrane surface in close proximity to the lipid glycerol backbone. Additionally, REDOR indicated contrasting recoupling efficiencies between biradicals. S/S_0 spectra for KL_4 [^{13}C]L12, [^{15}N]L17 displayed no significant dephasing in the presence of cholesterol-AMUPol, a consequence of shortenedT_2 relaxation in the presence of cholesterol-AMUPol.

Conclusions

Our preliminary results show different behavior between cholesterol-AMUPol and AMUPol for DNP of membrane peptide KL_4. We hypothesize these effects are attributed to biradical membrane partitioning and the electronic environment. We plan to further characterize the relationship between biradical membrane localization and DNP efficiency with electron T_1/T_2 measurements and the effects of biradical on membrane structure with ^{31}P NMR. We aim to characterize important features of biradicals in lipid membranes that allow simultaneous DNP and use of pulse sequences involving mixing times on the order of ~10-80msec.

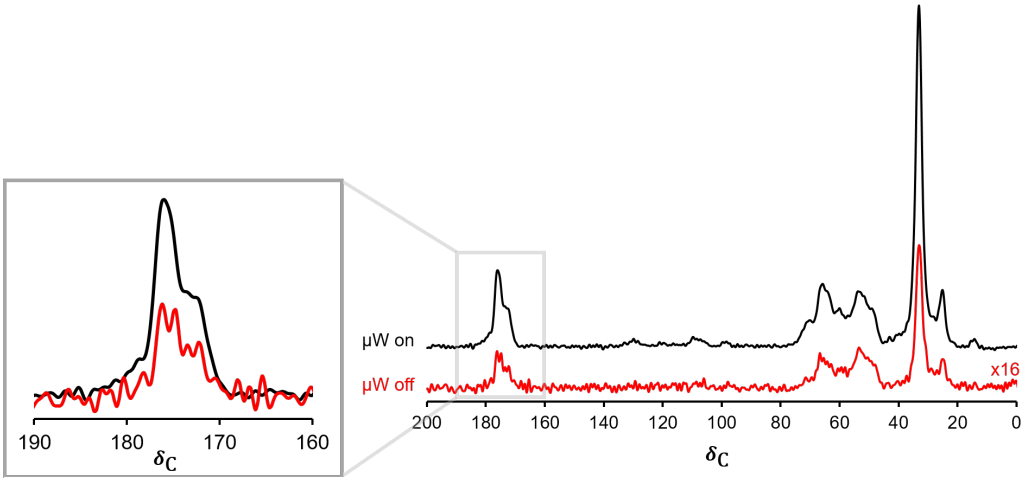

Fig. ^{13}C CP spectra with microwaves on (black) and microwaves off (red) for 2 mol% KL_4 [1-^{13}C]L12, [1-^{13}C]L13 in 5.5/2.7/2/1 DPPC-d_{62}/DPPC/POPG/cholesterol-AMUPol liposomes, corresponding to 10 mM biradical concentration. Resonances are observed for lipid functional groups: lipid terminal methyl (10-18 ppm), lipid sp^3 carbon (28-38 ppm), lipid glycerol backbone (45-80 ppm), lipid sp^2 carbon (125-135 ppm) and lipid carbonyl (168-174 ppm). (Boxed) ^{13}C enriched KL_4 carbonyl resonance at 176 ppm.

Acknowledgements

The National High Magnetic Field Laboratory is supported by the National Science Foundation through NSF/DMR-1157490/1644779 and the State of Florida. Additional support provided by NIH/BRS S10OD018519 and NIH/NIGMS P41GM122698.